Available online at **www.joac.info**

ISSN: 2278-1862

Journal of Applicable Chemistry

2021, 10 (6): 872-879

(International Peer Reviewed Journal)

The Effect of pH on the Synthesis and Characterization Hydroxyapatite from Bamboo Shell *(Sollen spp.)* with Emulsion Method

Wulandari, Diana Vanda Wellia and Novesar Jamarun*

Department of Chemistry, Faculty of Mathematics and Natural Sciences,
Andalas University, Padang, West Sumatera, **INDONESIA**
Email: novesarjamarun@sci.unand.ac.id

Accepted on 19th November, 2021

ABSTRACT

The present study, reports synthesizes of hydroxyapatite (HAp) material from bamboo shell waste (Sollen spp.) as Ca^{2+} ions biosource. The HAp was synthesized through emulsion method, using Span20, Tween80, and cyclohexane as the surfactants and oil phase. X-Ray Diffraction, Fourier Transform Infrared, and Scanning Electron Microscope-Energy Dispersive X-Ray characterizations were carried out to reveal the effect of pH on the synthesized HAp material. The XRD pattern confirmed that single-phase HAp was formed at pH 9, 10, and 11. Using the Scherrer equation, the smallest crystal size was 5.30 nm at pH 10. The SEM-EDS results showed the HAp had morphology with agglomerated particles with a Ca/P ratio of 1.82. Overall characterization results showed that pH had an insignificant effect on the crystallinity and morphology.

Graphical abstract

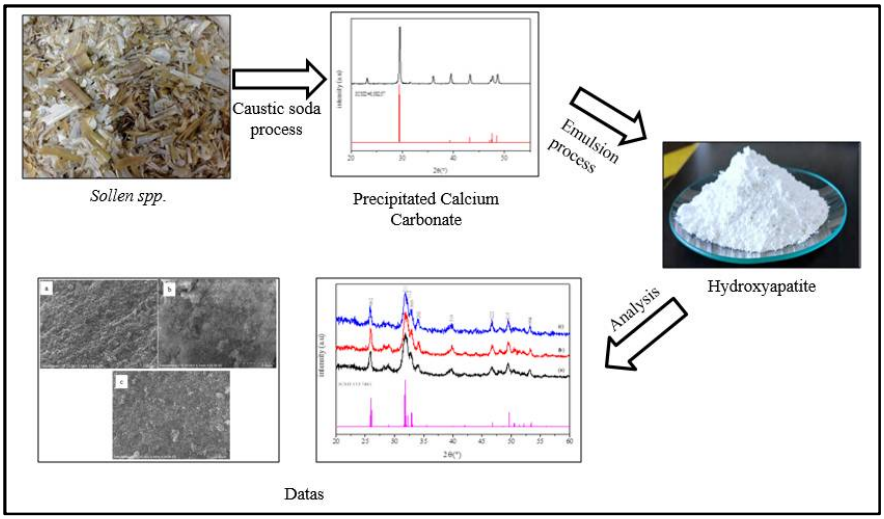

Keywords: Hydroxyapatite, *Sollen spp.*, Precipitated calcium carbonate, Emulsion method.

INTRODUCTION

In the last decade, nanomaterials have been researched on recently for their application in the biology, electronics, optics, transportation, and information technology fields. One particular nanomaterial that has been widely studied is hydroxyapatite (HAp) [1]. HAp, or $Ca_{10}(PO_4)_6(OH)_2$, is the main inorganic composition in human bone tissue [2], making it one of the most attractive biomaterials used for bone implants owing to its biological similarity and composition to human tissue [3]. Furthermore, HAphas great tissue bioactivity and the ability to bind directly to the bone to promote good osteointegration,resulting in it being favoredin orthopedics and dentistry [3], bone tissue engineering [4], drug delivery materials, and cell imaging [2].

Synthetic HAphas been widely prepared from natural sources (biosources) such as limestone [5], blood clamshells [6], golden snails, animal bones, among others. It also can be prepared from chemical substances as a source of calcium and its phosphates such as $CaCO_3$ and H_3PO_4 [7], $Ca(NO_3)_2$ and $(NH_4)_2HPO_4$ [8], $Ca(NO_3)_2.4H_2O$ and KH_2PO_4 [4].Several methods are used in the synthesis of HAp, such as precipitation [5], hydrothermal [6], double diffusion technique [9], sol-gel [10], biomimetics [11], and electrode position techniques [12]. These methods are expected to be able to produce Hap with nano-sized particles. Nanoparticles (1 nm = 10^{-9}m) provide opportunities for broader applications as they have properties that are not found in large particles. The use of nanomaterials has many advantages and provides added value to a material, such as achieving efficient, economic, and environmentally friendly technological advances [5].

Although several approaches have been carried out to control the size, shape, and crystallinity, some parameters that affect the particles size and shape of this material still need to be studied further. The emulsion method is a traditional method that has many advantages, includes high efficiency in controlling the shape and size of particles so that they are nano-sized [1]. Jarudilokkul *et al.* reported that Hap nanoparticles that were smaller than 70 nm had been successfully synthesized using the emulsion method with $CaCl_2$, $2H_2O$, and $(NH_4)_2HPO_4$ as precursors, caproic acid as oil phase, and Span 20 and Tween 80 as non-ionic surfactants [13]. Several other studies have also used the emulsion method to synthesize Hap nanoparticles and obtained various nano sizes, including 18–25 nm[3], 30–50 nm [1], and 20–100 nm [14]. This emulsion method is cheap and only requires simple tools, and can be more economical if the calcium source is a natural source (biosource) such as bamboo shell waste (*Sollen spp.*). In this study, this emulsion method is expected to produce uniformly sized and shaped Hap nanoparticles. This research will investigate the effect of pH on the crystallinity and morphology of HAp. Bamboo shells, Span 20, Tween 80, and cyclohexane were used as a source of calcium ion, non-ionic surfactant, and oil phase, respectively, in this HAp synthesis.

MATERIALS AND METHODS

Material: Diammonium hydrogen phosphate $(NH_4)_2HPO_4$, cyclohexane, Span20, Tween80, ethanol 96%, ammonia 25%, nitric acid (HNO_3) 65% were analytical grade and purchased from Merck. A bamboo shell sample was collected from Padang, Sumatera Barat.

Synthesis of CaO from bamboo shell waste: The bamboo shell sample was washed in water and dried in the sun before being crushed and sieved into powder form with a size 90 mesh. The powder was then calcined at 900^{o}C for 5 h to obtain CaO powder as follows: [6]

$$2CaCO_3 + \text{heat} \rightarrow 2CaO + 2CO_2$$

Synthesis of precipitated calcium carbonate (PCC): The PCC was synthesized by using a modified caustic soda method. A 5.6 g of CaO powder was dissolved into 9 mL of 2M HNO_3 and 191 mL of aqua bides before stirring with a stirrer for 10 min at 65°C with 400 rpm speed. The solution was then filtered, and the filtrate was collected and added with 150 mL of 1.5 M Na_2CO_3 solution at a flow rate

of 2.5 mL min^{-1}. The reaction was continued for 60 min at a stirring speed of 400 rpm. The solution was then filtered to obtain the PCC, which was calcined at 900°C and used as a precursor for the synthesis of HAp.

Synthesis of Hap by emulsion method: To prepare the emulsion, 0.705 g $(NH_4)_2HPO_4$ was dissolved in 15 mL of distilled water to obtain the aqueous phase. Span20 and Tween 80 were then mixed in a 1:1 ratio into 20 mL of cyclohexane at 250 rpm speed at room temperature to get the oil phase. Next, the aqueous phase was added to the oil phase and stirred at 250 rpm (solution I). Meanwhile, 0.5 g of CaO was dissolved in 10 mL of 2M HNO_3 (solution II) in another container and was mixed with solution I to form a w/o emulsion. Ammonia was added to the emulsion to obtain pH 9, 10, and 11 and agitated for 24 h. After agitation, the emulsion was washed with ethanol and distilled water. The precipitate was dried at 110^{o}C for 5 hours and calcined at 600^{o}C for 5 h This procedure was modified from an article by Jarudilokkul *et al.*[**13**].

Characterizations: Using XRF (PAN alytical), the amount of calcium in bamboo shell powder was analyzed. Then, the crystallinity of the Hap was characterized using XRD (XPERT PRO PAN alytical). The morphology and chemical composition of the Hap nanoparticles were observed and analyzed using SEM (Hitachi Flexsem) and EDX (Ametex EDAX). Meanwhile, the chemical interactions on the Hap nanoparticles were analyzed using FTIR (Perkin Elmer).

RESULTS AND DISCUSSION

Bamboo shell waste as Ca^{2+} ions biosource: Based on table 1, the X-Ray Fluorescence (XRF) characterization shows the bamboo shell has a high calcium content of 97.279%, indicating it is a good source of calcium in synthesis PCC [**15**] to form hydroxyapatite.

Table 1. The results of X-Ray Fluoresence (XRF) characterization

Component	Composition (%)
CaO	97,279
SiO_2	0,317
Al_2O_3	0,447
P_2O_5	0,587
Fe_2O_3	0,093
K_2O	0,007
CuO	0,004
MnO	0,005
Others	1,261

The structural analysis of PCC: In Figure 1, the X-Ray Diffraction (XRD) pattern of PCC obtained from the bamboo shells (*Sollen spp.*) shows the formation of PCC with a calcite structure based on ICSD data number 158257, where calcite is a stable phase at room temperature. The PCC was calcined at 900°C and used as a precursor for the synthesis of HAp.

Synthesis of HAp using w/o emulsion method: In general, the synthesis of Hap with the w/o emulsion method is achieved through three steps. First, diammonium hydrogen phosphate solution is dispersed into cyclohexane as the oil phase. Second, the oil phase is separated from the aqueous phase through agitation, and finally, residues such as cyclohexane, ammonium, and surfactants are removed.

When a surfactant is dissolved in cyclohexane, the surfactant molecules will form a structure that minimizes surface tension and surfactant assembly as a nanoreactor. Phosphate precursor is then added to this surfactant solution and then adsorbed on the surface of the surfactant assembly owing to hydrogen bonds between the hydrogen in the hydrophilic group of the surfactant and the oxygen in the phosphate ion [**16**]. Then, a calcium precursor solution is added to bind calcium to the surface of

the surfactant assembly to form a calcium phosphate layer (HAp). During the agitation process, HApis formed on the surface of the surfactant assembly, and then it is separated from the oil phase. The surfactant is then removed with distilled water, ethanol, and thermal decomposition in the air (calcination) [**17**].

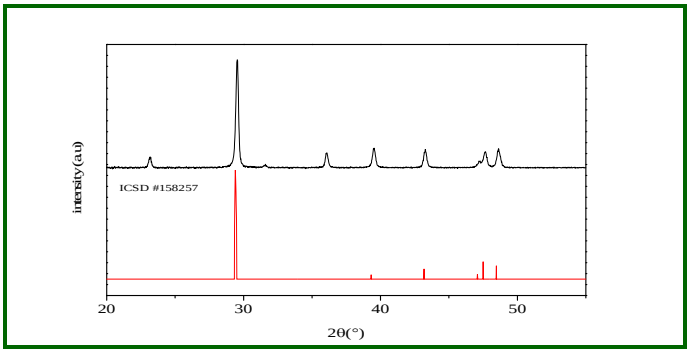

Figure 1. X-ray diffraction patterns of Precipitated Calcium Carbonate (PCC)

Synthesis of HAp using w/o emulsion method: In general, the synthesis of Hap with the w/o emulsion method is achieved through three steps. First, diammonium hydrogen phosphate solution is dispersed into cyclohexane as the oil phase. Second, the oil phase is separated from the aqueous phase through agitation, and finally, residues such as cyclohexane, ammonium, and surfactants are removed.

When a surfactant is dissolved in cyclohexane, the surfactant molecules will form a structure that minimizes surface tension and surfactant assembly as a nanoreactor. Phosphate precursor is then added to this surfactant solution and then adsorbed on the surface of the surfactant assembly owing to hydrogen bonds between the hydrogen in the hydrophilic group of the surfactant and the oxygen in the phosphate ion [**16**]. Then, a calcium precursor solution is added to bind calcium to the surface of the surfactant assembly to form a calcium phosphate layer (HAp). During the agitation process, HApis formed on the surface of the surfactant assembly, and then it is separated from the oil phase. The surfactant is then removed with distilled water, ethanol, and thermal decomposition in the air (calcination) [**17**].

Characterization to investigate the effect of pH on the crystallinity and morphology of Hap Analysis of XRD: In this study, Hap was synthesized in pH 9, 10, and 11. Figure 2 shows the formation of single-phase HAp and all samples have characteristic diffraction patterns according to ICSD number 157481 at 25.96°, 31.86°, 32.16°, 32.46°, 34.08°, 39.86°, 46.78°, 49.48°, 53.28° with index main (hkl): (002), (211), (112), (300), (202), (310), (222), (213), and (004), respectively [**18-21**].

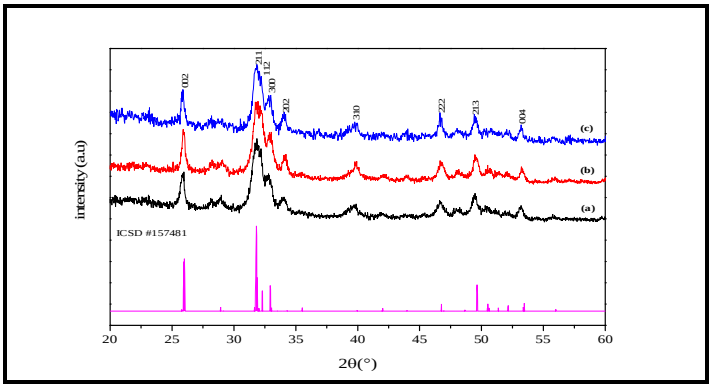

Figure 2. X-ray diffraction patterns of hydroxyapatite calcinated

at 600°C for 5 h at pH 9 (a) , pH 10 (b), pH 11 (c).

The XRD results in figure 2 show that Hap can be formed in the three pH conditions. Palanivelu *et al* stated that the reaction for the formation of Hap could be formed at alkaline pH (9 and 11) owing to the high interaction between Ca^{2+} and PO_4^{3-} ions.In contrast, a neutral pH (pH = 7) gives an inactive reactive medium, resulting in slowCa^{2+} ions and PO_4^{3-}interaction and this tends to lead to the formation of calcium-deficient HAp [**22**]. However, at higher pH conditions (> pH 11),Hap purity tends to decrease owing to the appearance of other minerals such as portlandite, $Ca(OH)_2$.
The Debye Scherrer equation determines the crystal size of the HAp.

$$D_{hkl} = \quad 0.9.\lambda\beta.\cos$$

where λ is the wavelength of the X-rays (1.5406 Å), θ is diffraction angle, full width at half maximum (FWHM) value **[23-24]**. From the Debye Scherrer equation, the Hap crystal sizes were calculated at 10.86 nm, 5.30 nm, and 6.9 nm for synthesized Hap at pH 9, pH 10, and pH 11, respectively. pH 10.0 was selected under our experimental conditions to obtain the HAp powder.

Analysis of Fourier Transform Infrared (FTIR): FTIR characterization is a method that observes the interaction of molecules with electromagnetic radiation in the 0.75–1,000 μm wavelength region or the 13,000–10 cm^{-1} wave number. Knowing the molecular interactions in the sample can confirm whether any material is formed or not.

Figure 3 shows the FTIR spectra of the HAp particles that were prepared at pH 9 (a), pH 10 (b), and pH 11 (c) and calcinated at 600°C for 5hours. The characteristic bands for PO_4^{3-} group appear at 452, 560, and 1023 cm^{-1} **[25-26]**. The peak at 452 cm^{-1} is attributed to theν_2 bending vibration of the phosphate group [**20**]. The strong peak observed in the 1023 cm^{-1} region is owing to the PO_4^{3-} group, while the peak at 560 cm^{-1} is attributed to theν_4 asymmetric bending vibrations mode of the O–P–O group [**27**]. This result corresponds to the XRD result, which indicates the presence of HAp.

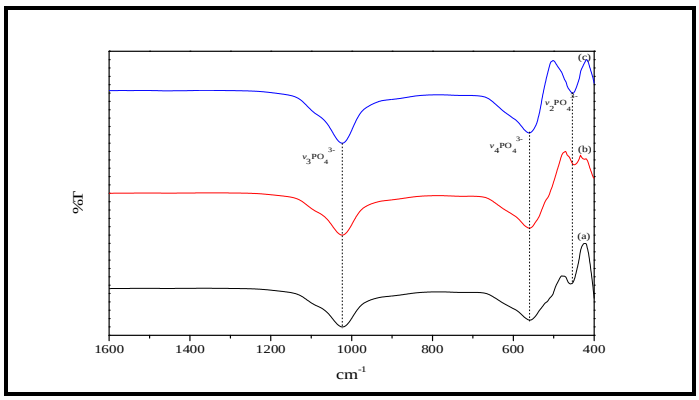

Figure 3. FTIR spectrum of hydroxyapatite calcinated at 600 °C for 5 h at pH 9 (a) , pH 10 (b), pH 11 (c).

Characterization of surface composition and morphology: SEM-EDS characterization was carried out to observe the surface morphology and determine the chemical composition of the elements on the surface of HAp. Figure 4(a–c) shows SEM images of Hap with variations in pH values. HAp with irregular shapes and agglomerated particles can be observed in all pH conditions [**28**] because at alkaline pH such as 9, 10, and 11, the mobility rate of Ca^{2+} and PO_4^{3-} ions is fast owing to the high kinetic energy that causes a fast collision, leading to agglomeration [**22**].

Figure 5 shows the EDS spectrum of the synthesized HAp. It shows Ca, P, and O as the constituent elements of HAp powder. Hap can be formed with a Ca/P ratio between 1.2 and 2 [**29**]. In this case, the Ca/P ratio of Hap is 1.82 and it is calcium-rich HAp.

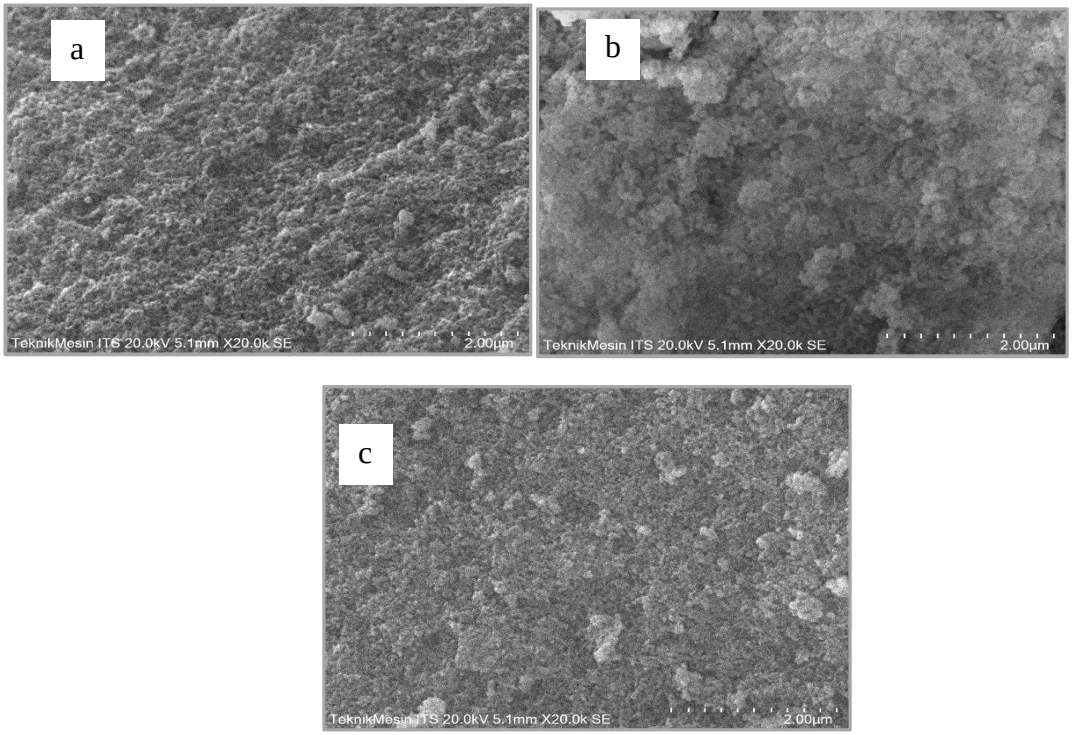

Figure 4. SEM image of hydroxyapatite calcinated at 600 °C for 5 h at pH 9 (a) , pH 10 (b), pH 11 (c).

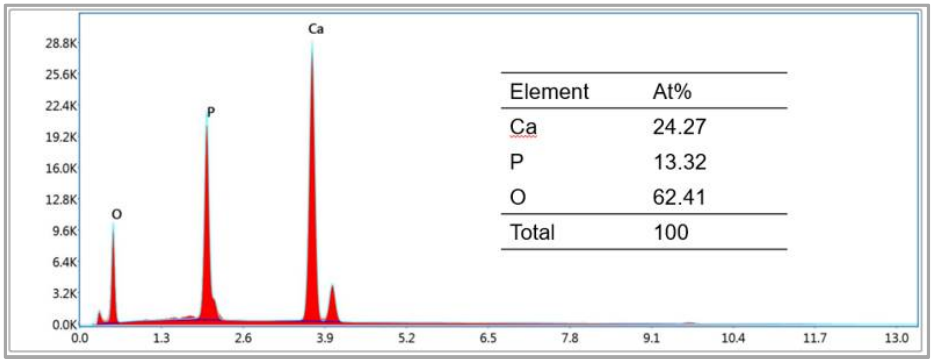

Figure 5. EDS spectrum of hydroxyapatite calcinated at 600 ^{o}C for 5 h at pH 10.

.

CONCLUSION

A biosource in the form of waste bamboo shells (*Sollen spp.*) has produced HAp with a high calcium source at 97,279% CaO. The optimal pH to synthesize HAp is under alkaline conditions of pH 9, 10, and 11. The XRD pattern and FTIR results confirmed that single-phase Hap was formed. The SEM-EDS results showed the HAp had morphology with agglomerated particles with a Ca/P ratio of 1.82. However, it is found that pH has no significant effect on the crystallinity and morphology of HAp.

ACKNOWLEDGMENT

The authors gratefully acknowledge financial support from the Ministry of Research, Technology and Higher Education (RISTEKDIKTI) of the Republic of Indonesia through the PMDSU Scholarship [Grant number 104/E4.1/AK.04.PT/2021]

REFERENCES

[1]. S. Bose, S.K. Saha, Synthesis and Characterization of Hydroxyapatite Nanopowders by Emulsion Technique, *Chem. Mater*., 2003. https://doi.org/10.1021/cm0303437.

[2]. X. Ma, Y. Chen, J. Qian, Y. Yuan, C. Liu, Controllable synthesis of spherical hydroxyapatite nanoparticles using inverse microemulsion method, *Mater. Chem. Phys.*, **2016**, 183,220–229. https://doi.org/10.1016/j.matchemphys.2016.08.021.

[3]. K. Saranya, M. Kowshik, S.R. Ramanan, Synthesis of hydroxyapatite nanopowders by sol-gel emulsion technique, *Bull. Mater. Sci.*, **2011**, https://doi.org/10.1007/s12034-011-0386-8.

[4]. B. B. Marija Prekajski Đorđevića, Jelena Maletaškića, Nadežda Stankovića, B. M. Katsumi Yoshidab, Toyohiko Yanob, In-situ immobilization of Sr radioactive isotope using nanocrystalline hydroxyapatite, *Ceram. Int.*, **2018**, 44, 1771–1777. https://doi.org/10.1016/j.ceramint.2018.03.170.

[5]. N. Jamarun, Z. Azharman, S. Arief, T. P. Sari, A. Asril, S. Elfina, Effect of temperature on synthesis of hydroxyapatite from limestone, *Rasayan J. Chem.*, **2015**.

[6]. Y. Azis, N. Jamarun, S. Arief, H. Nur, Facile synthesis of hydroxyapatite particles from cockle shells (Anadaragranosa) by hydrothermal method, *Orient. J. Chem*., **2015**. https://doi.org/10.13005/ojc/310261.

[7]. V. Stanić, D. Janaćković, S. Dimitrijević, S.B. Tanasković, M. Mitrić, M.S. Pavlović, A. Krstić, D. Jovanović, S. Raičević, Synthesis of antimicrobial monophase silver-doped hydroxyapatite nanopowders for bone tissue engineering, *Appl. Surf. Sci.*, **2011**, 257 4510–4518. https://doi.org/10.1016/j.apsusc.2010.12.113.

[8]. G. Guo, Y. Sun, Z. Wang, H. Guo, Preparation of hydroxyapatite nanoparticles by reverse microemulsion, *Ceram. Int.*, **2005**, 31 869–872. https://doi.org/10.1016/j.ceramint.2004.10.003.

[9]. A. R. Kumar, S. Kalainathan, Growth and characterization of nano-crystalline hydroxyapatite at physiological conditions, *Cryst. Res. Technol*., **2008**. https://doi.org/10.1002/crat.200711094.

[10]. P. Layrolle, A. Ito, T. Tateishi, Sol-Gel Synthesis of Amorphous Calcium Phosphate and Sintering into Microporous Hydroxyapatite Bioceramics, *J. Am. Ceram.*, Soc., **2005**. https://doi.org/10.1111/j.1151-2916.1998.tb02499.x.

[11]. S. Türk, Altınsoy, G. ÇelebiEfe, M. Ipek, M. Özacar, C. Bindal, Microwave–assisted biomimetic synthesis of hydroxyapatite using different sources of calcium, *Mater. Sci. Eng. C.*, **2017**. https://doi.org/10.1016/j.msec.2017.03.116.

[12]. M. Shirkhanzadeh, Direct formation of nanophase hydroxyapatite on cathodically polarized electrodes, *J. Mater. Sci. Mater. Med.*, **1998**. https://doi.org/10.1023/A:1008838813120.

[13]. S. Jarudilokkul, W. Tanthapanichakoon, V. Boonamnuayvittaya, Synthesis of hydroxyapatite nanoparticles using an emulsion liquid membrane system, Colloids Surfaces A Physicochem, *Eng. Asp.*, **2007**. https://doi.org/10.1016/j.colsurfa.2006.09.038.

[14]. K. Sonoda, T. Furuzono, D. Walsh, K. Sato, J. Tanaka, Influence of emulsion on crystal growth of hydroxyapatite, in: *Solid State Ionics*, **2002**. https://doi.org/10.1016/S0167-2738(02)00730-0.

[15]. R. J. and J. R. Novesar Jamarun, Sirly Yuwan, Synthesis And Characterization Carbonate Apatite From Bukit Tui Limestone, Padang, Indonesia, *J. Appl. Chem.*, **2015**, 4, 542–549.

[16]. S. K. Saha, A. Banerjee, S. Banerjee, S. Bose, Synthesis of nanocrystalline hydroxyapatite using surfactant template systems: Role of templates in controlling morphology, *Mater. Sci. Eng. C*., **2009**, 29 2294–2301. https://doi.org/10.1016/j.msec.2009.05.019.

[17]. S. Hajimirzaee, S. Chansai, C. Hardacre, C.E. Banks, A.M. Doyle, Effects of surfactant on morphology, chemical properties and catalytic activity of hydroxyapatite, *J. Solid State Chem*., **2019**, 276, 345–351. https://doi.org/10.1016/j.jssc.2019.05.031.

[18]. Y. Sun, G. Guo, D. Tao, Z. Wang, Reverse microemulsion-directed synthesis of hydroxyapatite nanoparticles under hydrothermal conditions, *J. Phys. Chem. Solids*., **2007**, 68, 373–377. https://doi.org/10.1016/j.jpcs.2006.11.026.
[19]. C. Yang, P. Yang, W. Wang, S. Gai, J. Wang, M. Zhang, J. Lin, Synthesis and characterization of Eu-doped hydroxyapatite through a microwave assisted microemulsion process, *Solid State Sci*., **2009**, 11, 1923–1928. https://doi.org/10.1016/j.solidstatesciences.2009.07.013.
[20]. A. Huang, H. Dai, X. Wu, Z. Zhao, Y. Wu, Synthesis and characterization of mesoporous hydroxyapatite powder by microemulsion technique, *J. Mater. Res. Technol*., **2019**, 8, 3158–3166. https://doi.org/10.1016/j.jmrt.2019.02.025.
[21]. Y. Sun, H. Yang, D. Tao, Microemulsion process synthesis of lanthanide-doped hydroxyapatite nanoparticles under hydrothermal treatment, *Ceram. Int.*, **2017**, 37, 2917–2920. https://doi.org/10.1016/j.ceramint.2011.03.030.
[22]. R. Palanivelu, A. Mary Saral, A. Ruban Kumar, Nanocrystalline hydroxyapatite prepared under various pH conditions, Spectrochim,. *Acta - Part A Mol. Biomol. Spectrosc*., **2014**, 131, 37–41. https://doi.org/10.1016/j.saa.2014.04.014.
[23]. M. Prekajski Đorđević, J. Maletaškić, N. Stanković, B. Babić, K. Yoshida, T. Yano, B. Matović, In-situ immobilization of Sr radioactive isotope using nanocrystalline hydroxyapatite, *Ceram. Int.*, **2018**, 44, 1771–1777. https://doi.org/10.1016/j.ceramint.2017.10.110.
[24]. G. E. Putri, S. Arief, F. R. G. , Novesar Jamarun, A. Fisli, Zilfa, and U. Septiani, Silica Mesoporous by Surfactant-Assisted Hydrothermal Method, *J. Appl. Chem*., **2017**, 6 , 1058–1068.
[25]. V. Collins Arun Prakash, I. Venda, V. Thamizharasi, E. Sathya, A comparative study on microemulsion synthesis of hydroxyapatite powders by ionic and Non-Ionic surfactants, Mater. Today Proc., **2020**. https://doi.org/10.1016/j.matpr.2020.10.026.
[26]. A. Changotra, R. Gupta, S. Paul, Selective Oxidation of Benzyl Alcohol Over Hydroxyapatite – Supported Au-Pd Nanoparticles, *J. Appl. Chem.*, **2014**, 3, 2014, 653–662
[27]. S. Akter Jahan, M.Y.A. Mollah, S. Ahmed, M. Abu Bin Hasan Susan, Nano-Hydroxyapatite Prepared from Eggshell-Derived Calcium-Precursor using Reverse Microemulsions as Nanoreactor, Mater, *Today Proc*., **2017**, 4, 5497–5506. https://doi.org/10.1016/j.matpr.2017.06.005.
[28]. F. Foroughi, S. A. Hassanzadeh-Tabrizi, A. Bigham, In situ microemulsion synthesis of hydroxyapatite-MgFe2O4 nanocomposite as a magnetic drug delivery system, *Mater. Sci. Eng. C*., 68, **2016**, 774–779. https://doi.org/10.1016/j.msec.2016.07.028.
[29]. A. Charlena, S. T. Bikharudin, Wahyudi, Erizal, Synthesis and characterization of hydroxyapatite-collagen-chitosan (Ha/Col/Chi) composite by using Ex-situ wet precipitation method, *Rasayan J. Chem*., **2017**, 10, 766–770. https://doi.org/10.7324/RJC.2017.1031768